Pergamon

PII: S0301-9322(96)00032-8

Int. J. Multiphase Flow Vol. 22, No. 5, pp. 883–891, 1996

0301-9322/96 $15.00 + 0.00

EFFECT OF INSERTED ROD AND CROSS FLOW ON TOP FLOODING OF PIPE

M. OSAKABE and H. FUTAMATA
Tokyo University of Mercantile Marine, 2-1-6 Etchujima Koutou-ku, Tokyo 135, Japan

(Received 26 October 1995; in revised form 19 April 1996)

Abstract—Flow pattern in flooding pipes can be considerably changed by inserting a rod or posing a cross flow at the top end. A non-uniform flow pattern around the circumference due to the inserted rod was observed in the present experiment. By increasing the diameter of the rod, a similar flow pattern as that in a thin rectangular channel was observed and the partial delivery flow rate could be predicted well with the correlation for the thin rectangular channel. The cross flow at the top end resulted in a non-uniform distribution of the water film around the pipe periphery. The partial delivery of water flow was decreased when the cross flow velocity was increased at a given gas velocity. The limitation mechanism for the cross flow energy of the delivery water was considered. Copyright © 1996 Elsevier Science Ltd.

Key Words: non-uniformity, top flooding, inserted rod, cross flow, thin rectangle, annulus, flow pattern, characteristic length, non-dimensional velocity, multiphase flow

1. INTRODUCTION

Flooding in countercurrent gas–liquid flow is an important phenomenon in industrial applications such as heat pipes, film separators and reflux condensers. In nuclear reactor systems, flooding is very important in connection with the operation of emergency core cooling systems (ECCS). Special interest is in the partial delivery behavior in the annular downcomer in pressurized water reactors (PWR) under loss-of-coolant accident (LOCA) conditions.

Previous studies on flooding can be classified into two categories. One is focused on the onset of flooding and another is focused on the partial delivery in countercurrent gas–liquid flow. In the present study, the partial delivery problem from a water pool or a cross flow above vertical pipes was studied. The gas is allowed to flow upward through the flooding pipe and the upper plenum or the duct above the pipe provides the water for penetration

The characteristics of the partial delivery phenomenon are dependent on various parameters such as passage geometries, properties of fluid and method of operation. The end geometries play an important role in determining the partial delivery flow rate. It is believed that the water flow rate is limited at the top end of the passage when enough water exists above it, so it is called top flooding. In this top flooding behavior, the characteristic length to represent and describe the flow pattern related to the end geometries should be properly defined.

Generally in the pipes, a liquid film flow along the wall and a gas flow in a central core can be observed in pipes. The top flooding behavior in pipes is characterized with the hydraulic diameter and can be predicted successfully with an analysis assuming an uniform film around the circumference (Richter 1981). However, annular passages can not be characterized by using the hydraulic diameter and the theoretical prediction assuming the uniform flow around the circumference did not seem to be appropriate (Osakabe *et al.* 1989). It was also pointed out that the top flooding behavior in the annular passage was similar to that in a thin rectangular channel. The flow pattern in the annular passage is significantly deformed due to the inserted rod and it becomes a similar flow pattern such as that in the thin rectangular channel.

The flow pattern at the top end geometry may be affected also by the flow in the water pool above the flooding pipes. In the previous study, the top flooding in pipes was studied under the condition of a stagnant water pool of constant depth. But strictly speaking, the stagnant condition was usually nominal because bubbles or plugs released from the flooding pipe and water supply

to the upper plenum might induce a flow in the water pool. The effect of the flow on the top flooding behavior has not been studied experimentally.

In the present study, the effect of an inserted rod and a cross flow on the top flooding in pipes was studied experimentally. The non-uniform flow pattern due to the inserted rod and the cross flow was carefully observed. The top flooding data were plotted by using the conventional method and the results were discussed in connection with the observed flow pattern.

2. PREVIOUS STUDY ON TOP FLOODING IN PIPES

Previous experiments on top flooding have resulted essentially in an empirical correlation. The correlation relates the gas and liquid fluxes under the top flooding condition. Wallis (1969) proposed,

$$j_G^{*1/2} + m j_L^{*1/2} = C. \quad [1]$$

The non-dimensional velocities are defined as;

$$j_i^* = \frac{\rho_i^{1/2} j_i}{[gD(\rho_L - \rho_G)]^{1/2}} \ (i = \text{L or G}), \quad [2]$$

where j: superficial velocity, ρ: density, D: hydraulic diameter, g: acceleration due to gravity and the suffix L: liquid, G: gas. The inner diameter is used as D for a round pipe. Bharathan *et al.* (1983) reported that C is 0.725 and m is 1.0 at a pipe diameter of 25 mm. Sudo *et al.* (1987) indicated C is approximately 0.7 and m is 1.0 at pipe diameters of 8, 12 and 20 mm. For the pipes of the small diameter, C and m are considered to be constant.

Richter *et al.* (1979) conducted a top flooding experiment in annuli with the outer diameter D_1 of 444.5 mm and the inner diameter D_2 of 393.7 mm, and $D_1 = 444.5$ mm/$D_2 = 342.97$ mm. When the average circumference W is used as the characteristic length, their results can be described with (Osakabe *et al.* 1989),

$$J_G^{*1/2} + 0.8 J_L^{*1/2} = 0.38 \quad [3]$$

where the non-dimensional velocity is defined as;

$$J_i^* = \frac{\rho_i^{1/2} j_i}{[gW(\rho_L - \rho_G)]^{1/2}} \ (i = \text{L or G}). \quad [4]$$

Nakamura *et al.* (1990) conducted a top flooding experiment in an annular passage of $D_1 = 220$ mm/$D_2 = 200$ mm. Their experimental results can be correlated with the following correlation, which is almost identical to [3]

$$J_G^{*1/2} + 0.78 J_L^{*1/2} = 0.37. \quad [5]$$

For the top flooding behavior in thin rectangular channels, Osakabe *et al.* (1994) used the test section with a wider span of 10–100 mm and a gap width of 2, 5 and 10 mm. The observation showed clearly the non-uniform distribution of the flow pattern in the span direction. The span length W was considered to be a key characteristic length. The experimental data were predicted well with the correlation using the span length as;

$$J_G^{*1/2} + 0.3 \mathrm{Bo}^{1/8} J_L^{*1/2} = 0.58 \quad [6]$$

where the Bond number (Bo) is defined as,

$$\mathrm{Bo} = gW^2(\rho_L - \rho_G)/\sigma$$

where σ is a surface tension. The characteristic length in the Bo number is the span length W. If 1/4 of the average circumference of the annuli is used as the characteristic length in [3] and [5], the value of C is approximately 0.54 which is nearly equal to the right hand side of [6]. This suggested the similar flow pattern around the circumference in annuli, just as in the thin rectangular channel (Osakabe *et al.* 1989).

3. EXPERIMENTAL APPARATUS AND PROCEDURE

Shown in figure 1 is a schematic of the air/water test apparatus to study the effect of an inserted rod. The apparatus consisted of a lower plenum, a test section and an upper plenum which were made of transparent acrylic resin for the observation of the flow patterns. The test section was 350 mm long and consisted of a pipe with an inner diameter of 50 mm. The diameter of the rod inserted into the test section could be varied, as 16, 30, 36, 40 and 45 mm. A parametric study of the test section length was not conducted in the present study because the experimental results by Sudo *et al.* (1987) had shown no dependency on the test section length for top flooding. Air was supplied to the test section from the lower plenum and discharged through the separator in the upper plenum. Water was supplied to the upper plenum and was collected in the lower plenum. The upper plenum was divided with a porous annulus into two regions. One included a weir to maintain the upper plenum water level, a water supply and a drain, and the other was connected to the protruding test section. The weir height was 50 mm higher than the top end of the test section to ensure enough water above the test section. The disturbance and the induced flow due to the water supply to the upper plenum was successfully reduced by the porous annulus. The lower plenum had a porous plate to fix the inserted rod and an air supply.

Shown in figure 2 is a schematic of the test apparatus to study the effect of cross flow. A duct of 40 × 40 mm cross-section was installed instead of the upper plenum. The test section was

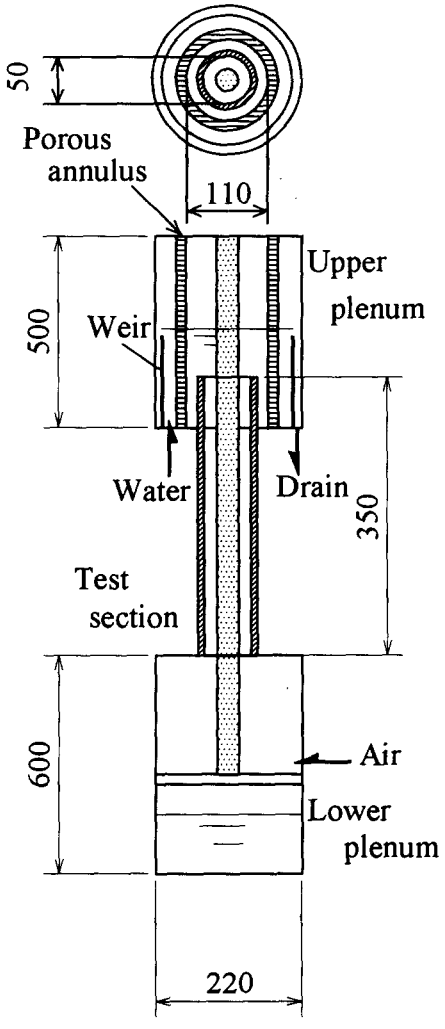

Figure 1. Experimental apparatus with inserted rod.

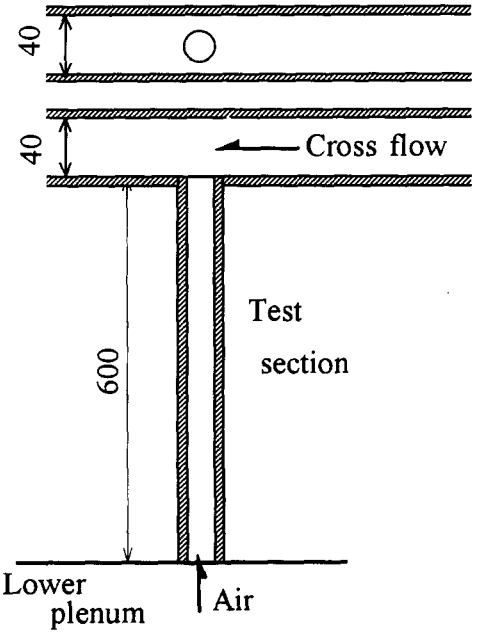

Figure 2. Experimental apparatus with cross flow duct.

600 mm long and consisted of a pipe with an inner diameter of 10 or 20 mm. The same lower plenum as that shown in figure 1 was used.

In the experiment, water was allowed to flow into the upper plenum or the cross flow duct, and was drained through the test section at a given air flow rate supplied from the lower plenum. The downward water flow rate was obtained by noting the time interval to accumulate a known level of water in the lower plenum.

4. EXPERIMENTAL RESULTS AND DISCUSSION

Effect of an inserted rod

Shown in figure 3 are the typical flow patterns in the pipe, annulus and thin rectangular duct. The average film thickness is uniform around the circumference of the pipe. Water was observed to mainly fall down at the two corner parts of the thin rectangular test section (Osakabe *et al.* 1994). Increasing the aspect ratio in the annular passage of the present study, "unit cells" around the circumference just as in the thin rectangular channel could be observed. The "unit cells" were not fixed and were moving around the circumference, and coalescence and separation of those could be observed. Thus it was impossible to define and clarify the number of "unit cells". Even when the gas velocity is high, the water falls down at one location of the circumference and a uniform film around the circumference could not be observed. The flow pattern in the annulus is quite different from that in the pipe.

Shown in figure 4 are the experimental results for the inserted rod with diameters of 16, 30, 36, 40 and 45 mm. In this figure, the non-dimensional velocities j_i^* (i = L or G), defined by [2] were calculated with the hydraulic diameter as the characteristic length. The data in the pipe without the inserted rod and with the inserted rod of 16 mm agree well with [1] using $C = 0.725$ and $m = 1.0$ based on the experimental results at the pipe diameter of 25 mm by Bharathan & Wallis (1983). The non-dimensional partial delivery flow rate based on the hydraulic diameter becomes larger with increasing the diameter of the inserted rod. By using the hydraulic diameter, it is impossible to describe all the present data with one correlation.

The hydraulic diameter is also not appropriate to correlate the data of non-uniform flow pattern as the size of the "unit cells" is sometimes larger than the hydraulic diameter itself. It is considered that the hydraulic diameter is appropriate when the flow pattern around the circumference is uniform, just as that of single phase flow. Since the distribution of void fraction and velocity around the circumference is considered to be important, the average circumference W is considered to be appropriate as the characteristic length. Shown in figure 5 are all the experimental results replotted with [4] by using the average circumference W defined as,

$$W = \pi(D_1 + D_2)/2. \qquad [7]$$

In the pipe without the rods, W of $\pi D_1/2$ is used as the characteristic length. Increasing the diameter of the inserted rod, the values of m and C decrease. It is noteworthy that the data obtained in pipes with the inserted rod diameter of 40 and 45 mm can be correlated with $C = 0.4$ and $m = 0.46$.

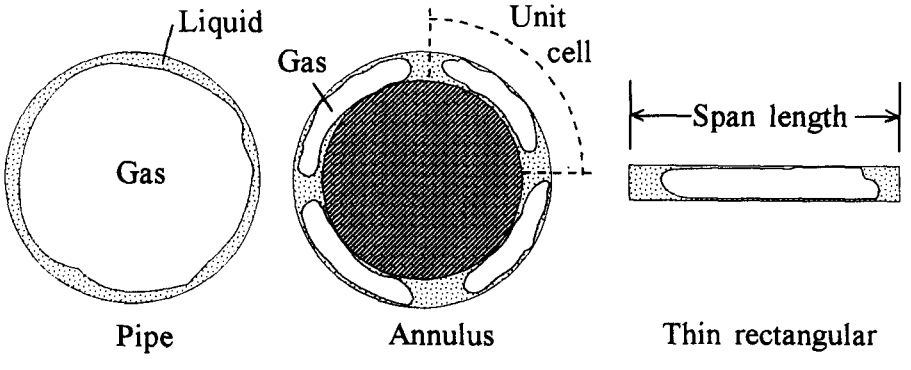

Figure 3. Typical flow patterns for pipe, annulus and thin rectangular channel.

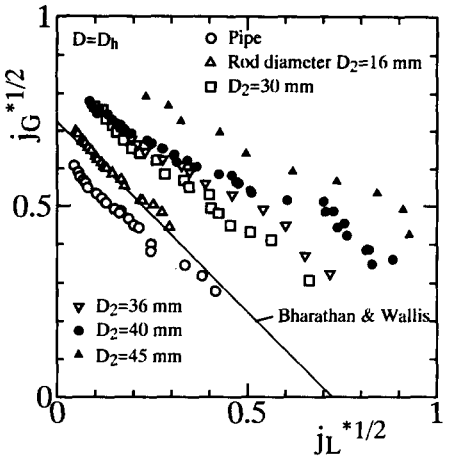

Figure 4. Experimental results in annuli by using the hydraulic diameter as the characteristic length in the non-dimensional velocity.

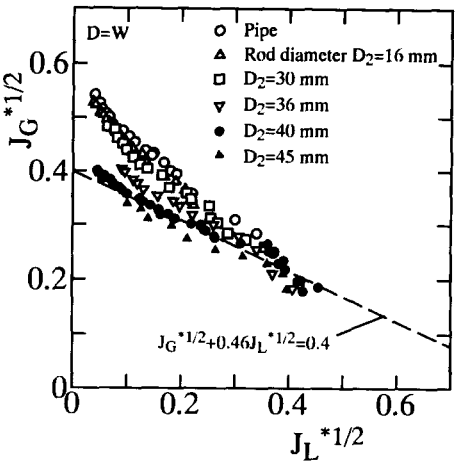

Figure 5. Experimental results in annuli by using the average circumference as the characteristic length in the non-dimensional velocity.

For further discussion, all the data in figure 5 are correlated with [1] and the constants m and C are obtained by the least squares methods. Shown in figure 6 is the relation between the aspect ratio W/R and the values of C obtained in the present experiment and the other top flooding experiments for annuli. The gap R is defined as $(D_1 - D_2)/2$. The value of C approaches 0.4 with increasing the aspect ratio. This value at high aspect ratios does not depend on the size of the annuli because the other experimental facilities from which the data in figure 6 are obtained, is much larger than the present apparatus. A representative full-sized reactor (PWR) has an annular downcomer with a gap width of 0.25 m and an average circumference of 14.4 m. The aspect ratio of the downcomer is 57.6. Bharathan (1979) summarized many scaled-down experiments for the downcomer of a PWR and also pointed out that the value of C is approximately 0.4 and does not depend on the relative size.

The value of C defined with the average circumference is approximately 0.4 and that defined with 1/4 circumference becomes 0.57. This value is nearly the same as that obtained in the thin rectangular channels as shown in [6]. Shown in figure 7 are the relation of Bo number and constants obtained in the thin rectangular channel and the annuli of the high aspect ratio. The data of the annuli are calculated with the characteristic length of 1/4 average circumference. The present data

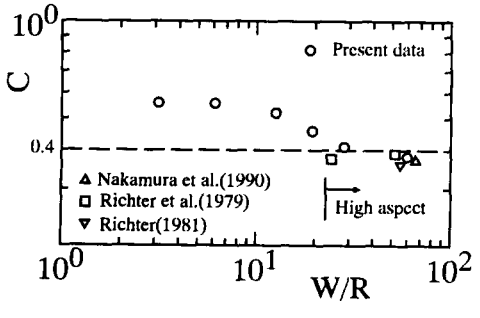

Figure 6. Relation of C and the aspect ratio W/R.

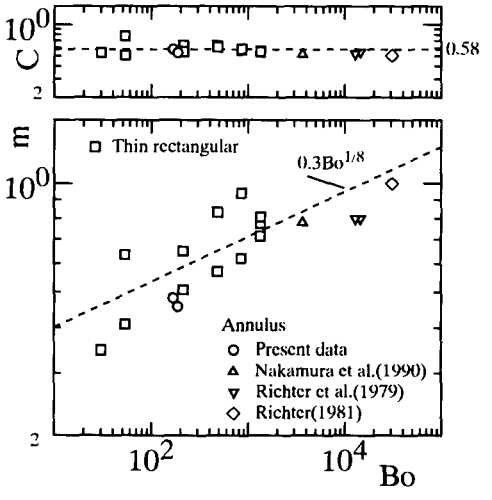

Figure 7. Relation of C and Bo number. (The characteristic length is 1/4 of the average circumference for annuli and the span length for the thin rectangular channel.)

in figure 7 are obtained in the high-aspect ratio experiments with a rod diameter of 40 and 45 mm, respectively. The value of C is constant and independent of the Bo number related to the span in the thin rectangular channel and 1/4 the average circumference in the annuli. The value of m for the annuli and the thin rectangular channels increases with the Bo number. The data for the annuli can be predicted well with the correlation obtained in the thin rectangular channels. The 1/8 power of the Bo number is derived from the transition mechanism of the characteristic length from the span length at the high gas velocity to the Taylor instability wave length λ, defined as

$$\lambda = 2\pi\left[\frac{\sigma}{g(\rho_L - \rho_G)}\right]^{1/2}, \qquad [8]$$

at the low velocity in the thin rectangular channel (Osakabe *et al.* 1994). When the gas velocity is high in the thin rectangular channels, the span W is an important characteristic length for representing the falling water at the two corner walls. But at the low gas velocity, randomly falling water at the central region of the span direction mitigates the role of W. The flooding behavior is strongly affected by the channel geometry at high gas velocities, but the effect of the geometry dwindles at low gas velocities and the behavior tends to depend only on the characteristics of the two-phase flow itself such as the Taylor instability length.

It is noteworthy that top flooding in annular passages can be characterized by using some fraction of the average circumference and the hydraulic diameter assuming uniform flow around the circumference does not seem to be appropriate. Variation of void fraction and velocity in the direction of the circumference are important for the top flooding mechanism in the annular passage just as in the top flooding in the thin rectangular passage. The non-uniform flow behavior in the annular passage was also reported for rising large bubbles which occupy almost the whole flow area (Griffith 1964; Barnea & Shemer 1986).

Effect of cross flow

Shown in figure 8 is a typical flow pattern at the top end of the test pipe with or without cross flow. The average film thickness around the circumference is uniform with a stagnant water pool above the flooding pipe. When a cross flow duct is installed above the flooding pipe, a thicker film can be observed at the downstream-side compared to that at the upstream-side. A non-uniform film around the circumference is generated with the cross flow.

When the cross flow velocity is zero, the top flooding is a simple phenomenon of mass exchange. In the cross flow condition as shown in figure 9, a part of the cross flow water is delivered into the flooding pipe. The horizontal cross flow velocity becomes zero when the water is delivered into the flooding pipe. On the other hand, the air released from the flooding pipe obtains a cross flow velocity. So in the top flooding at the cross flow condition, not only the mass but also the cross flow energy is exchanged at the top end of the flooding pipe. It is considered that the energy exchange is conducted at the top end of the pipe and is affected with the pipe geometry. So as a

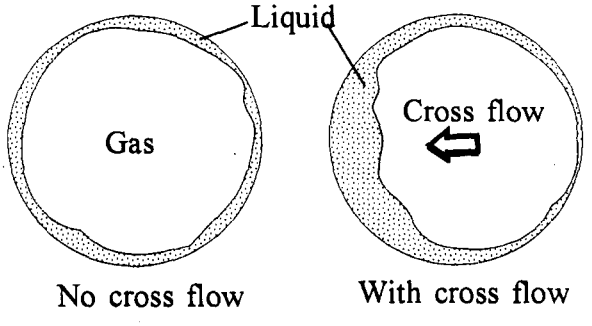

Figure 8. Typical flow patterns for pipes with or without cross flow.

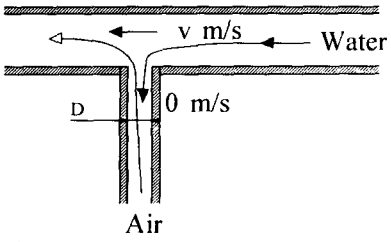

Figure 9. Exchange of mass and cross flow energy.

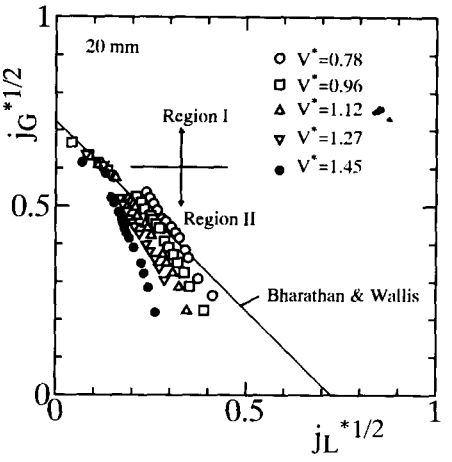

Figure 10. Experimental results in pipe of 20 mm diameter with cross flow.

first attempt, the non-dimensional cross flow velocity related to the energy exchange is defined by using the diameter of flooding pipe as,

$$V^* = \frac{\rho_L^{1/2} V}{[gD(\rho_L - \rho_G)]^{1/2}} \quad [9]$$

where V is the cross flow velocity at the duct. Shown in figure 10 are experimental results using a flooding pipe with a diameter of 20 mm for five different cross flow velocities. The data can be classified into the region I and II. The effect of cross flow is relatively small and the data agree well with the correlation by Bharathan and Wallis (1983) in region I. In region II, a smaller partial delivery water flow rate is obtained with an increase in the cross flow velocity. This is probably due the fact that the film thickness in region I is relatively small compared to that in region II and the non-uniform film effect is negligible in region I. The thicker film increases the interfacial shear stress significantly (Wallis 1969). So in region II, it is possible that the thick film at the downflow side significantly reduces the water flow rate. The stronger non-uniformity due to the higher cross flow velocity results in the smaller delivery of water. Shown in figure 11 are experimental results using a flooding pipe with a diameter of 10 mm. The data can be classified into the same two regions as in figure 10. It is clear that the cross flow effect is negligible in region I. A smaller delivery of water occurs due to the higher cross flow velocity in region II.

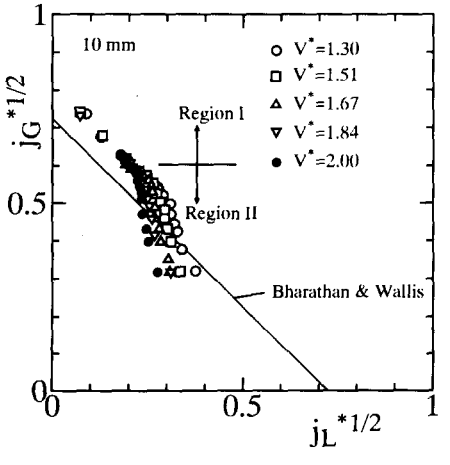

Figure 11. Experimental results in pipe of 10 mm diameter with cross flow.

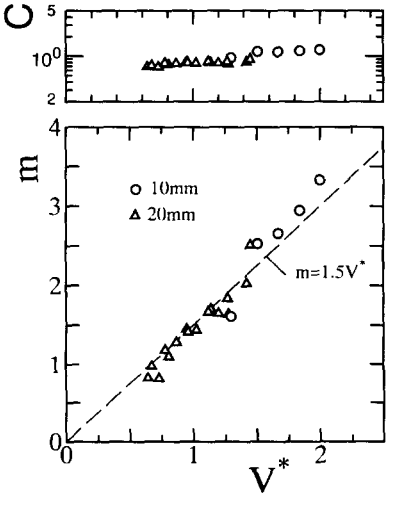

Figure 12. Relation of m, C and the non-dimensional cross flow velocity.

All the region II data in figures 10 and 11 are correlated with [1] and the constants m and C are obtained by the least squares methods. Shown in figure 12 is the relation of the non-dimensional cross flow velocity V^* and the constants. The value of C is approximately constant and independent of V^* but the constant m depends linearly on V^*. The value of m can be correlated with,

$$m = 1.5V^*. \qquad [10]$$

The linear relation [10] gives very interesting correlation for the cross flow energy in the present experimental range. Substituting [10] into [1],

$$j_G^{*1/2} + 1.5\sqrt{2}E_L^{*1/2} = C \qquad [11]$$

where E_L^* is defined as;

$$E_L^* = \frac{1}{2}\mathrm{V}^{*2}j_L^* \qquad [12]$$

and it is considered to be the non-dimensional cross flow energy of the water delivered into the flooding pipe. Increasing the cross flow velocity at a given gas velocity, decreases the partial delivery of water to maintain a certain value of E_L^*. The penetration of the water with the high cross flow energy is suppressed at the top end of the flooding pipe. It seems to be very interesting and reasonable that [11] gives the limitation for the cross flow energy of the delivery water because not only the mass but also the cross flow energy is exchanged at the top end.

5. CONCLUSION

Top flooding experiments in a pipe with an inserted rod and a cross flow were conducted. The following results relating to the two-phase non-uniformity were obtained.

Effect of the inserted rod

(1) By using the average circumference as the characteristic length, the value of C approached 0.4 with increasing the diameter of the inserted rod. This value did not depend on the size of the annuli.
(2) The non-uniform distribution of void fraction and velocity in the direction of the circumference is important for the top flooding mechanism in the annular passage just as in top flooding in thin rectangular passages. Increasing the aspect ratio in annular passages, several "unit cells" around the circumference appeared and the characteristic length became some fraction of the average circumference W.
(3) By using 1/4 average circumference as the characteristic length in the high aspect ratio annuli, the flooding data could be described well with the correlation for the thin rectangular channel.

Effect of the cross flow

(1) When the cross flow duct was installed above the flooding pipe, a thicker film could be observed at the downstream-side compared to that in the upstream-side. The non-uniform film around the circumference was generated with the cross flow. The stronger non-uniformity due to the higher cross flow velocity resulted in smaller partial delivery of water.
(2) The flooding data with the cross flow could be classified into two regions I and II. The effect of the cross flow was relatively small and the data agreed well with the previous correlation in region I. In region II, the smaller partial delivery of water was obtained at the higher cross flow velocity. Increasing the cross flow velocity at a given gas velocity, decreases the partial delivery water due to the limitation for the cross flow energy of the delivery water.

REFERENCES

Barnea, D. & Shemer, L. 1986 Rise velocity of large bubbles in stagnant liquid in non-circular ducts. *Int. J. Multiphase Flow* **12,** 1025–1027.

Bharathan, D. 1979 Air–water countercurrent annular flow, EPRI NP-1165.

Bharathan, D. & Wallis, G. B. 1983 Air–water countercurrent annular flow. *Int. J. Multiphase Flow* **9,** 349–366.

Griffith, P. 1964 The prediction of low-quality boiling voids. *J. Heat Transfer* **86,** 327–333.

Nakamura, H., Koizumi, Y., Anoda, Y. & Tasaka, K. 1990 Air–water two-phase flow in large vertical annuli. *Proc. of 27th National Heat Transfer Symposium of Japan*, pp. 964–966 (in Japanese).

Osakabe, M. & Kawasaki, Y. 1989 Top flooding in thin rectangular and annular passages. *Int. J. Multiphase Flow* **15,** 747–754.

Osakabe, M., Kubo, T. & Baba, H. 1994 Top flooding in thin rectangular channels. *JSME Int. J.* **B37,** 491–496.

Richter, H. J., Wallis, G. B. & Speers, M. S. 1979 Effect of scale on two-phase countercurrent flow flooding, NUREG/CR-0312.

Richter, H. J. 1981 Flooding in tubes and annuli. *Int. J. Multiphase Flow* **7,** 647–658.

Sudo, Y., Usui, T. & Kaminaga, M. 1987 Study on countercurrent flow limiting in the vertical channel(I). *Proc. of 24th National Heat Transfer Symposium of Japan*, pp. 446–448 (in Japanese).

Wallis, G. B. 1969 *One-dimensional Two Phase Flow*. McGraw Hill, New York.